Investigation of the Reaction of Partial Oxidation of Methane over Ni/La2O3 Catalyst

ARTICLE *in* ENERGY & FUELS · SEPTEMBER 2006

Impact Factor: 2.79 · DOI: 10.1021/ef0602729

Investigation of the Reaction of Partial Oxidation of Methane over Ni/La_2O_3 Catalyst

Matthieu Fleys,[†] Yves Simon,[†] Dariusz Swierczynski,[‡] Alain Kiennemann,[‡] and Paul-Marie Marquaire*,[†]

Département de Chimie Physique des Réactions, UMR 7630 CNRS−INPL, 1 rue Grandville, B.P. 451 F-54001 Nancy Cedex, France, and Laboratoire des Matériaux, Surfaces et Procédés pour la Catalyse, CNRS−Université Louis Pasteur, 25 rue Becquerel, F-67087 Strasbourg, France

Received June 14, 2006. Revised Manuscript Received August 22, 2006

The reaction of the partial oxidation of methane was investigated over Ni/La_2O_3 catalysts prepared by impregnation. Two different reactors were used, a perfectly jet-stirred reactor and a fixed-bed reactor. The influences of nickel content, calcination temperature, reaction temperature, residence time, and contact time were investigated. Mechanistic information was derived from the comparison of the results obtained in both reactors. Characterization techniques such as X-ray diffraction, temperature-programmed oxidation, temperature-programmed reduction, and transmission electron microscopy were used to assess the state of the catalyst prior to and after the reaction.

1. Introduction

Natural gas is expected to play an increasing role in coming decades as a fuel of choice because of decreasing oil reserves. The conversion of natural gas into valuable chemicals remains extremely meaningful. Methane can be converted into synthesis gas, a mixture of hydrogen and carbon monoxide, via three main reactions: the dry reforming reaction (1), the water reforming reaction (2), and partial oxidation (3). These reactions lead to different H_2/CO ratios.

$$CH_4 + CO_2 = 2CO + 2H_2 \qquad \Delta_r H^0_{(298K)} = +247 \text{ kJ mol}^{-1} \tag{1}$$

$$CH_4 + H_2O = CO + 3H_2 \qquad \Delta_r H^0_{(298K)} = +206 \text{ kJ mol}^{-1} \tag{2}$$

$$CH_4 + \frac{1}{2}O_2 = CO + 2H_2 \qquad \Delta_r H^0_{(298K)} = -38 \text{ kJ mol}^{-1} \tag{3}$$

The partial oxidation of methane (POM) has two major advantages; the expected H_2/CO ratio is 2, which is close to the optimal ratio for the low-temperature Fischer−Tropsch reactions to paraffinic liquid, and it is mildly exothermic so a reactor based on this reaction would be more energy-efficient than that for the reforming reactions. Moreover, oxidation reactions are much faster than reforming reactions, so a small reactor could yield high throughput.[1]

Many different catalysts such as metal oxides, supported or unsupported metals, metal carbides, and sulfides have been extensively studied for these reactions. A lot of work was devoted to nickel-based catalysts for their low price, but nickel catalysts tend to favor carbon deposition and catalyst deactivation. Hence, significant work was done on the support or on catalyst precursors such as perovskites or solid solutions[2,3] in order to avoid or limit carbon deposition.[4−8] Moreover, from these studies, it appears that basic support[9] and strong interaction between the active phase and the support[10] can limit carbon deposition. Taking into account the literature results, nickel supported on lanthanum oxide was chosen in this study for its good performance and stable activity.

The reaction mechanism of the catalytic partial oxidation of methane still remains unclear, and a unified viewpoint has not been reached up to now. The mechanism can proceed either via the direct way where CO and H_2 are produced as primary products[6,11−16] or via the indirect way where methane combustion produces CO_2 and H_2O followed by steam and CO_2 reforming of the remaining methane.[4,17−20]

* Author to whom correspondence should be addressed. Phone: +33 383 175 070. Fax: +33 383 378 120. E-mail: Paul-Marie.Marquaire@ensic.inpl-nancy.fr.

[†] Département de Chimie Physique des réactions, UMR 7630 CNRS−INPL.

[‡] Laboratoire des Matériaux, Surfaces et Procédés pour la Catalyse, CNRS−Université Louis Pasteur.

(1) Bharadwaj, S. S.; Schmidt, L. D. *Fuel Process. Technol.* **1995**, *42*, 109−127.

(2) Provendier, H.; Petit, C.; Estournes, C.; Kiennemann, A. *Appl. Catal., A* **1999**, *180*, 163−173.

(3) Yamazaki, O.; Tomishige, K.; Fujimoto, K. *Appl. Catal.* **1996**, *136*, 49−56.

(4) Diskin, A. M.; Cunningham, R. H.; Ormerod, M. *Catal. Today* **1998**, *46*, 147−154.

(5) Chen, P.; Zhang, H.-B.; Lin, G.-D.; Tsai, K.-R. *Appl. Catal.* **1998**, *166*, 343−350.

(6) Lu, Y.; Xue, J.; Yu, C.; Liu, Y.; Shen, S. *Appl. Catal., A* **1998**, *174*, 121−128.

(7) Slagtern, A.; Schuurman, Y.; Leclercq, C.; Verykios, X. E.; Mirodatos, C. *J. Catal.* **1997**, *172*, 118−126.

(8) Leroi, P.; Madani, B.; Pham-Huu, C.; Ledoux, M.-J.; Savin-Poncet, S.; Bousquet, J. L. *Catal. Today* **2004**, *91−92*, 53−58.

(9) Kuś, S.; Otremba, M.; Taniewski, M. *Fuel* **2003**, *82*, 1331−1338.

(10) Barbero, J.; Peña, M. A.; Campos-Martin, J. M.; Fierro, J. L. G.; Arias, P. L. *Catal. Lett.* **2003**, *87*, 211−218.

(11) Hu, Y. H.; Ruckenstein, E. *Catal. Lett.* **1995**, *34*, 41−50.

(12) Hu, Y. H.; Ruckenstein, E. *J. Catal.* **1996**, *158*, 260−266.

(13) Ruckenstein, E.; Hu, Y. H. *Appl. Catal., A* **1999**, *183*, 85−92.

(14) Tulenin, Y. P.; Sinev, M. Y.; Savkin, V. V.; Korchak, V. N. *Catal. Today* **2004**, *91−92*, 155−159.

(15) Chu, Y.; Li, S.; Lin, J.; Gu, J.; Yang, Y. *Appl. Catal.* **1996**, *134*, 67−80.

(16) Au, C. T.; Wang, H. Y. *J. Catal.* **1997**, *167*, 337−345.

(17) Tsipouriari, V. A.; Zhang, Z.; Verykios, X. E. *J. Catal.* **1998**, *179*, 283−291.

10.1021/ef0602729 CCC: $33.50
Published on Web 09/26/2006 PAGE EST: 8.2

In this work, the influence of nickel content, calcination temperature, and operating conditions on the reaction performances and products distribution is reported using two different reactors, a perfectly jet-stirred reactor (PSR) and a fixed-bed reactor (FB). The results provide some insights about the mechanistic discussion.

Moreover, it is shown that the frontier between the direct and the indirect mechanism is not fixed and mainly depends on the operating conditions. This frontier is probably less significant than what is usually expected.

2. Experimental Procedure

2.1. Catalyst Preparation and Characterization Techniques. The Ni/La_2O_3 catalysts were prepared by impregnating La_2O_3 powder (Alfa Aesar, 99%) with a nickel nitrate solution at 1.0 M [$Ni(NO_3)_2$, $6H_2O$, 99.9%, Aldrich]. Different nickel contents were obtained by adding the appropriate volume of solution. The impregnated samples were kept at ambient temperature for 5 h. Then, they were dried at 110 °C for 1 h. Finally, the dried powder was calcined at 800 °C for 5 h in the air. The nominal content of nickel ($x Ni/La_2O_3$) is expressed in weight percent; x varies between 0.16 and 9.4%.

The specific areas of the samples were obtained at 77 K using a Sorptometer Coulter SA 3100. Transmission electron microscopy (TEM) investigations were carried out using a TOPCON-EM002B apparatus coupled with an energy dispersion X-ray analyzer operating at 200 kV. X-ray powder diffraction (XRD) patterns were recorded on a Siemens D-5000 powder diffractometer using nickel-filtered Cu Kα radiation (1.5406 Å).

Temperature-programmed reduction (TPR) with a thermal conductivity detector (TCD) and temperature-programmed oxidation (TPO) with a mass spectrometer were conducted using a conventional apparatus. For each sample, 50 mg of the corresponding powder was placed in a U-shaped quartz tube (6.0 mm internal diameter). Reduction profiles were obtained by heating the samples from 25 to 900 °C at 15 °C min^{-1} in a 3% H_2-N_2 mixture flowing at 50 mL min^{-1}. Oxidation profiles were obtained by heating the samples from 20 to 790 °C at 15 °C min^{-1} in a 5% O_2-He mixture flowing at 50 mL min^{-1}.

The Ni and C contents of the solids were measured by elemental analysis performed at the Laboratoire Central d'Analyse, CNRS, in Vernaison, France.

2.2. Description of the Reactors. Two different reactors were used in this work: a PSR and a FB.

2.2.1. The PSR. The PSR was used to investigate the mechanism of the reaction, taking into account both surface reactions and gas-phase reactions. The PSR was designed according to the Matras et al.'s criteria[21,22] in order to get a well-stirred gas-phase volume without mass and thermal gradients. The mixing was ensured by the kinetic energy of the gas arriving in a cross-shaped injector with four nozzles at its branched extremities.

A schematic representation of the reactor is given in Figure 1. The reactor was hemispherical (diameter = 3 cm and volume = 110 cm^3). Catalyst powder was pressed into cylindrical pellet at 1.6 kbar. Each pellet weighted 0.45 g and had a 12 mm diameter and a 1 mm thickness. The compression profile was monitored by a computer in order to get identical pellets. Up to eight catalyst pellets could be loaded in the reactor. The pellets were laid on the surface of a removable cylindrical quartz support. This support was

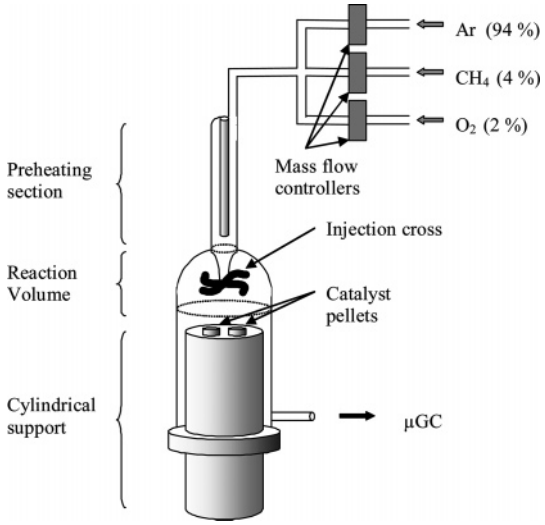

Figure 1. Schematic representation of the catalytic jet-stirred reactor.

heated by Thermocoax resistance wires so that the temperature of the catalyst and the gas-phase temperature were the same.

Before entering the reactor, the reactant mixture was preheated. The temperature of the first preheating part was 100 °C lower than the reactor temperature, while the temperature of the second preheating part was equal to the one of the reactor. The temperature of the gas phase, called the reaction temperature, was measured thanks to a thermocouple located inside a quartz finger at the middle of the free volume.

2.2.2. The FB. The FB was mainly used for testing catalyst performances. In this reactor (internal diameter = 4 mm), the catalyst powder was held on quartz wool. The reactor was heated by Thermocoax resistance wires located at the immediate contact of the quartz wall. Calcined samples were pelletized and sieved at a particle size in the range 0.5−0.7 mm. The amount of catalyst powder in the reactor was varied from 100 to 300 mg. For 100 mg of the catalyst, the corresponding bed height was equal to 5 mm.

2.2.3. Operating Conditions. The feed composition (vol %) was $CH_4/O_2/Ar$ = 4:2:94. The reactants were highly diluted in argon in order to control the temperature and avoid hot spots.[23] The operating pressure was constant and equal to 800 mm of Hg (107 kPa) for both reactors. The outlet composition was analyzed by an on-line gas chromatograph (Agilent 3000 A Micro GC) equipped with TCDs. The major compounds detected were H_2, CO, and CO_2, while the minor ones were C_2H_6, C_2H_4, and C_2H_2, denoted as C_2.

The residence time of the gas phase (τ) in the PSR was calculated according to

$$\tau = \frac{V}{Q(T_r,P_r)} \tag{4}$$

where V is the gas-phase volume and $Q(T_r,P_r)$ is the total flow rate (cm^3/s) calculated at the temperature and the pressure of the reaction.

The contact time (t_c) was equal to

$$t_c = \frac{W}{Q(T_r,P_r)} \tag{5}$$

where W is the catalyst weight (g).

Selectivities of CO and H_2 were calculated according to

$$S_{CO} = \frac{CO}{CO + CO_2 + 2(C_2H_6 + C_2H_4 + C_2H_2)} \tag{6}$$

which is close to

(18) Ito, M.; Tagawa, T.; Goto, S. *J. Chem. Eng. Jpn.* **1999**, *32* (3), 274−279.
(19) Dissanayake, D.; Rosynek, M. P.; Kharas, K. C. C.; Lunsford, J. H. *J. Catal.* **1991**, *132*, 117−127.
(20) Prettre, M.; Eichner, C.; Perrin, M. *Trans. Faraday Soc.* **1946**, 42, 335−340.
(21) David, R.; Matras, D. *Can. J. Chem. Eng.* **1975**, *53*, *3* (3), 297−300.
(22) Matras, D.; Villermaux, J. *Chem. Eng. Sci.* **1973**, *28*, 129−137.
(23) Boucouvalas, Y.; Zhang, Z. L.; Verykios, X. E. *Catal. Lett.* **1994**, *27* (1−2), 131−142.

$$S_{CO} = \frac{CO}{CO + CO_2} \quad (7)$$

and

$$S_{H_2} = \frac{H_2}{2X_{CH_4}CH_4^{in}} \quad (8)$$

where X_{CH_4} is the methane conversion and CH_4^{in} is the methane content at the inlet of the reactor.

In the relationships 6−8, concentrations are expressed in molar percent.

3. Results and Discussion

3.1. Influence of the Preparation Method on the Catalytic Activity. *3.1.1. Influence of the Calcination Temperature.* From sections 3.1−3.4, all experiments were carried out using the PSR. The reaction was performed at 750 °C using one catalyst pellet (0.45 g of 1.39Ni/La_2O_3) at a residence time equal to 3 s. The results are reported in Table 1. When the calcination temperature was lower than 800 °C, no influence on the conversions and the selectivities was observed. But at 900 °C, the catalyst performances were reduced drastically. Methane conversion was changed from 0.22 to 0.12 and H_2 selectivity decreased from 0.67 to 0.50 when the calcination temperature increased from 800 to 900 °C. A high calcination temperature favors catalyst sintering; nickel particles tend to aggregate leading to a decrease of the particle dispersion and a decrease of the catalytic activity. In the following, all samples were calcined at 800 °C, and the reaction temperature range was comprised between 500 and 800 °C.

3.1.2. Influence of the Nickel Content. The reaction was carried out at 750 °C and $\tau = 3$ s for 5 h. Table 2 summarizes the expected compositions from calculations and the real nickel composition determined by elemental analysis prior to and after the reaction. From this table, it appears that the expected nickel contents are very close to the real nickel loadings of the fresh samples. Moreover, comparing nickel loading prior to and after the reaction shows that the differences remain within the range of reproducibility error. Hence, on the basis of these results, no nickel loss was observed after the reaction.

The catalytic performances at 750 °C, $\tau = 3$ s using one catalyst pellet, are shown in Figure 2. Conversions and selectivities increase sharply with nickel loading when $0.16 < x < 2$. Then, the catalytic activity is stabilized despite the increase of nickel loading. Hence, it is clear that catalytic properties do not evolve proportionally with the nickel content. Nickel dispersion may reach a limited value as nickel loading increases. It is also noteworthy that, although H_2 and CO concentrations increase with nickel loading, the ratio H_2/CO keeps decreasing when $0.16 < x < 2$ and finally stabilizes at 1.8.

The influence of nickel content on carbon deposition was investigated using two different catalyst, $x = 1.39\%$ and $x = 6.98\%$. The POM reaction was performed at 700 °C, $\tau = 3$ s, for 10 h using one catalyst pellet. When $x = 1.39\%$, the amount of deposited carbon was 0.35 wt %, while it was equal to 1.24 wt % for $x = 6.98\%$. It implies that carbon deposition increases with the nickel content.[18]

In the following, all of the experiments were performed using the 1.39Ni/La_2O_3 catalyst calcined at 800 °C. This catalyst was chosen for its relatively good activity and low carbon deposition, an essential point to avoid catalyst deactivation.

3.2. Characterization of the Catalyst. Characterization analyses were done using 1.39Ni/La_2O_3 calcined at 800 °C. The analyses were performed on the catalyst prior to the reaction ("fresh") and after the reaction at 700 °C for 10 h ("used").

The Brunauer−Emmett−Teller (BET) area of the fresh catalyst was equal to 12.5 $m^2\ g^{-1}$, while the one of the used catalyst was 8.5 $m^2\ g^{-1}$. These values are quite low, and the specific area decrease is attributed to the particles' sintering phenomenon, which may occur during the reaction, and to the modification of the support as shown by XRD. To a smaller extent, the reduction of the BET area may also result from the carbon deposition on the catalyst surface.

XRD analyses are given in Figure 3. The XRD pattern of the fresh sample exhibits peaks corresponding to $La(OH)_3$ and $La(OH)CO_3$ but also to the perovskite structure $NiLa_2O_4$, while the XRD pattern of the used sample exhibits peaks corresponding to $La(OH)_3$ and La_2O_3. During the POM reaction, $NiLa_2O_4$ may be transformed into Ni^0/La_2O_3 as suggested by Choudhary et al.[24] It is interesting to note that no peaks related to Ni or NiO were detected because of the small amount of nickel loading in the catalyst. It is therefore necessary to use electronic microscopy to observe nickel crystallites.

TPR analyses are shown in Figure 4. Looking at the fresh sample, two peaks, α and β, can be observed at 410 and 710 °C, respectively. The first peak, α, was attributed to NiO reduction into Ni, while the second one, β, was attributed to hydroxy or oxycarbonate reduction. It is noteworthy that these two peaks are much smaller for the used catalyst, indicating that the catalyst was reduced during the POM reaction. A small peak can be observed for the fresh sample at 2000 s; it may be related to the reduction of the $NiLa_2O_4$ perovskite.[25]

Figure 5 shows TPO of the used sample. Two maximums can be found for the CO and CO_2 productions. The first one appears at 740 °C, while the second one appears at 790 °C. It suggests that there are two different types of solid carbon which deposited during the POM reaction. The first peak may be attributed to the carbon nanotubes oxidation, while the second peak is due to very structured carbon such as the graphitic type. The possible oxidation of the CH_x surface species at a lower temperature does not seem to happen on the basis of this experiment. It is noteworthy that CO does not come from the oxidation process but is due to the CO_2 fragmentation in the mass spectrometer. Indeed, the CO and CO_2 peaks appear at the same temperature, and the ratio between the maximums of the CO_2 and the CO peaks is the same. Moreover, CO_2 may come from the carbon oxidation and from the oxycarbonates decomposition. In POM experiments at 700 °C, the amount of oxycarbonates should be minimized because the temperature is high enough and the composition of the reactional mixture is not appropriate for oxycarbonates formation. Assuming that CO_2 only comes from deposited carbon, the amount of solid carbon formed during the POM reaction was found to be equal to 0.6 mg, which corresponds to 1.2 wt %. This low value is on the same order of magnitude as the one determined by elemental analysis.

Figure 6 shows the TEM analyses of the used sample. Nickel particles are dispersed in the lanthanum oxide matrix. After reaction, the average size of the nickel particles is equal to about 10−20 nm (see Figure 6a). Moreover, TEM analysis shows that nickel particles are surrounded by a continuous layer of around 1 nm thickness (Figure 6b). Corresponding energy dispersive

(24) Choudhary, V. R.; Uphade, B. S.; Belhekar, A. A. *J. Catal.* **1996**, *163*, 312−318.
(25) Ruckenstein, E.; Hu, Y. H. *J. Catal.* **1996**, *161*, 55−61.

Table 1. Influence of the Calcination Temperature on the Products Distribution (T = 750 °C, One Pellet, Ni wt % = 1.39, τ = 3 s)

calcination temperature (°C)	methane conversion X_{CH4}	oxygen conversion X_{O2}	CO selectivity S_{CO}	H_2 selectivity S_{H_2}	H_2/CO
600	0.22	0.40	0.70	0.67	1.8
700	0.22	0.44	0.71	0.67	1.8
800	0.21	0.41	0.66	0.67	1.9
900	0.12	0.34	0.47	0.50	2.1

Table 2. Elemental Analysis of Nickel Loading in the xNi/La_2O_3 Catalysts[a]

wt % Ni (expected)	0.18	0.46	0.94	1.44	1.96	4.28	7.06	10.46
wt % Ni (real − before reaction)	0.16	0.40	0.90	1.39	1.80	4.28	6.98	9.34
wt % Ni (real − after reaction)	0.165	0.38	0.88	1.35	1.80	4.02	7.00	9.05

[a] Analyses were done prior to reaction and after reaction at 750 °C, τ = 3 s over 5 h.

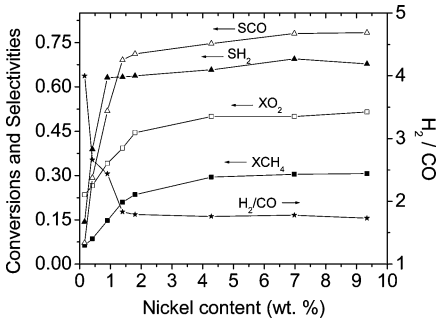

Figure 2. Influence of nickel content on the catalyst performances. All samples were calcined at 800 °C while the reaction was performed at T = 750 °C and τ = 3 s using one pellet.

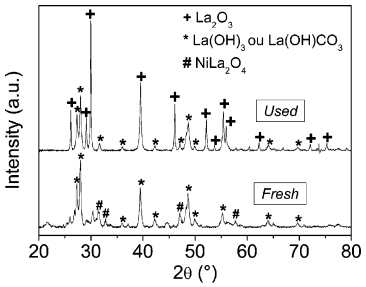

Figure 3. XRD patterns of the fresh and used 1.39Ni/La_2O_3 catalyst.

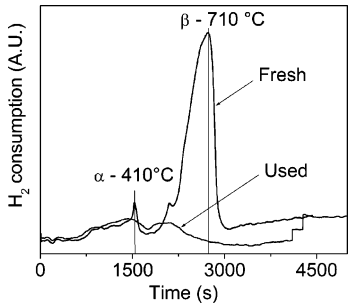

Figure 4. TPR profiles of the fresh and used 1.39Ni/La_2O_3 catalyst.

X-ray analyses show that the overlayer contains lanthanum and nickel. This thin interface between nickel and lanthana was observed by Slagtern et al.,[7] and it could explain the stable and active performances of the catalyst.[26,27] Figure 6c shows the formation of multiwall carbon nanotubes at the surface of the catalyst, which tend to curve in the upper part of the figure.

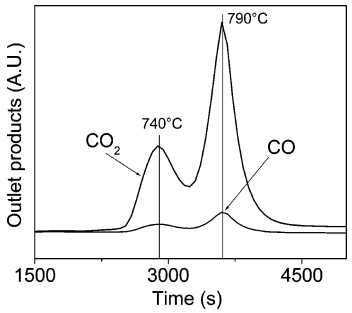

Figure 5. TPO profile of the used 1.39Ni/La_2O_3 catalyst.

3.3. Stability of the 1.39Ni/La_2O_3 Catalyst. *3.3.1. Stability of the Catalytic Performances.* The stability of the 1.39Ni/La_2O_3 catalyst was investigated at 750 °C, τ = 8s, using one catalyst pellet. The stability test was performed at τ = 8s in order to get a higher contact time between the gas mixture and the catalyst surface which corresponds to more severe conditions. The results are given in Figure 7. The catalyst shows a very good stability over 120 h. Methane and oxygen conversion stabilizes around 40% and 60%, respectively, while hydrogen and carbon monoxide selectivities are equal to 0.7 and 0.78, respectively. The H_2/CO ratio is about 1.8, which is slightly inferior to the stoichiometric ratio of the partial oxidation of methane reaction. It shows that global reaction 3 is not the only reaction and that other side reactions, such as reaction 1, occur at the same time. The carbon balance is about 95%. Excellent stability of the Ni/La_2O_3 catalysts was previously observed by various authors for the partial oxidation of methane[17] or the CO_2 reforming of methane.[26,28,29]

3.3.2. Catalyst Behavior during Temperature Cycles. The influence of temperature on the 1.39Ni/La_2O_3 catalyst was studied by considering temperature reacting cycles. For a given cycle, temperature was continuously increased from 500 to 800 °C and then decreased from 800 to 500 °C. Three consecutive cycles were performed, and the methane conversion is reported as a function of temperature in Figure 8. The reaction was performed at τ = 8s, using one catalyst pellet. The catalyst pellet was not prereduced before the reaction.

Cycle 1 shows an important hysteresis loop, as already observed in the literature.[15,30,31] Between 500 and 700 °C, methane conversion is found to be lower when the temperature increases than when it decreases. Interestingly, the lower part

(26) Zhang, Z.; Verykios, X. E.; MacDonald, S. M.; Affrossman, S. *J. Phys. Chem.* **1996**, *100*, 744−754.
(27) Requies, J.; Cabrero, M. A.; Barrio, V. L.; Güemez, M. B.; Cambra, J. F.; Arias, P. L.; Pérez-Alonso, F. J.; Ojeda, M.; Peña, M. A.; Fierro, J. L. G. *Appl. Catal., A* **2005**, *289*, 214−233.
(28) Tsipouriari, V. A.; Verykios, X. E. *J. Catal.* **1999**, *187*, 85−94.
(29) Zhang, Z. L.; Verykios, X. E. *Appl. Catal.* **1996**, *138*, 109−133.
(30) Slagtern, A.; Swaan, H. M.; Olsbye, U.; Dahl, I. M.; Mirodatos, C. *Catal. Today* **1998**, *46*, 107−115.
(31) Provendier, H.; Petit, C.; Estournes, C.; Kiennemann, A. *Stud. Surf. Sci. Catal*. **1998**, *119*, 741−746.

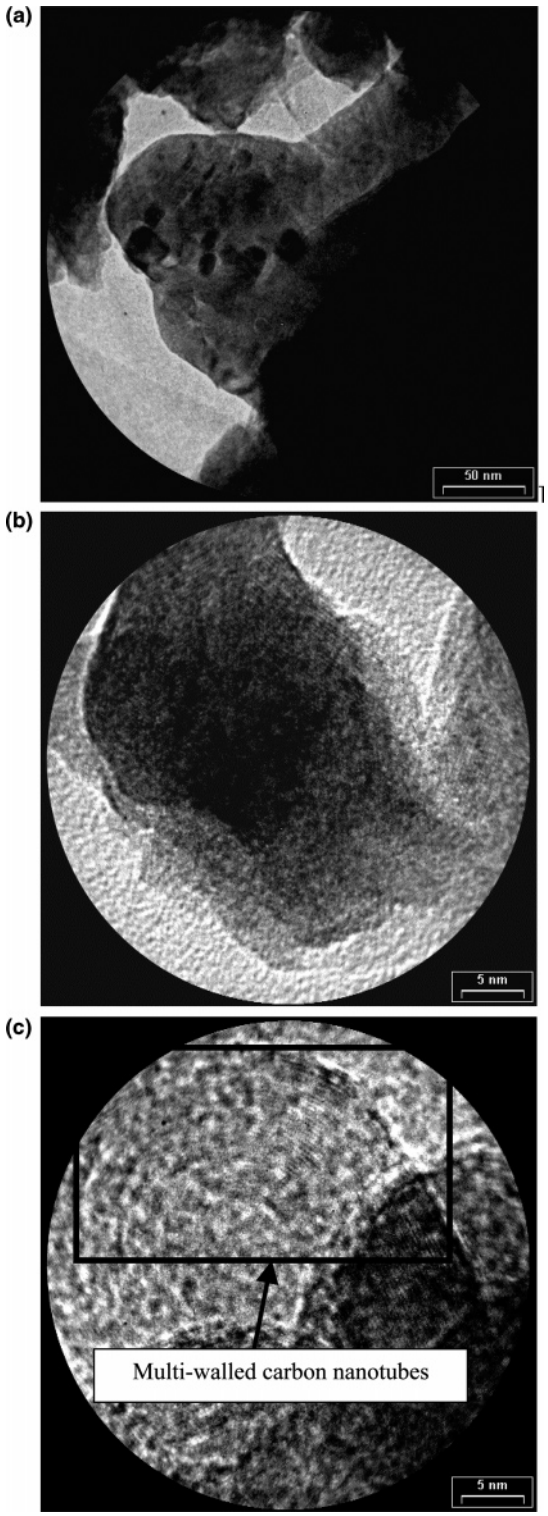

Figure 6. TEM pictures of the used 1.39Ni/La$_2$O$_3$ catalyst. (a) Scale = 50 nm catalyst particles. (b) Scale = 5 nm, overlayer. (c) Scale = 5 nm, carbon deposition.

of the curve in cycles 2 and 3 corresponding to the increasing temperature is getting closer to the upper part of the curve corresponding to the decreasing temperature. Moreover, it is noteworthy that the upper curve remains identical for all cycles. These results can be explained on the basis of redox reactions. Initially, nickel oxide is present on the catalyst surface, but as the temperature increases, it is reduced into metallic nickel. The reduction process NiO → Ni^0 happens between 500 and 700 °C. It was reported by many authors that Ni^0 is active for syngas production while NiO favors the total oxidation products, H_2O and CO_2.[14,15,19,32,33] Hence, when the temperature decreases from 700 to 500 °C, the initial state of nickel is metallic nickel, which explains the high activity. Of course, when the temperature is decreasing, the catalyst can be reoxidized by gaseous or surface oxygen. That is why a hysteresis can still be observed on cycles 2 and 3. But it appears that the reoxidizing process is getting a smaller importance with the cycle number. Furthermore, it is not excluded that the increasing temperature tends to activate irreversibly the nickel particle and independently of the redox reactions. Finally, the fact that no difference is observed between 700 and 800 °C implies that the nickel valence is constant over this temperature range.

In the following sections, the data presented are obtained at stable conditions, after cycle 3.

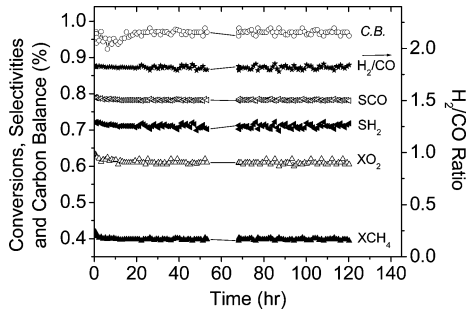

Figure 7. Stability study of the 1.39Ni/La$_2$O$_3$ catalyst at 750 °C and τ = 8 s, using one pellet.

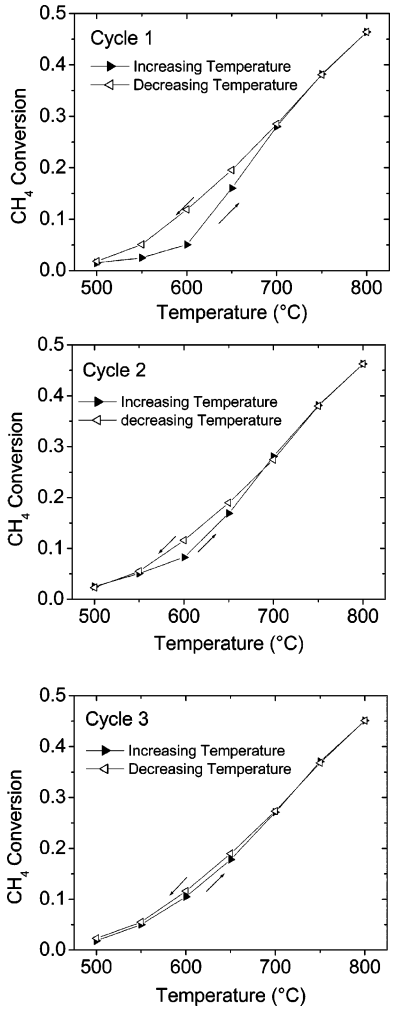

Figure 8. Temperature cycles over the 1.39Ni/La$_2$O$_3$ catalyst, at τ = 8 s, using one pellet.

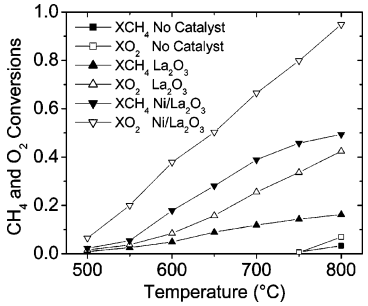

Figure 9. Oxygen and methane conversions as a function of temperature without the catalyst, with four pellets of La_2O_3 and four pellets of $1.39Ni/La_2O_3$ at $\tau = 3$ s.

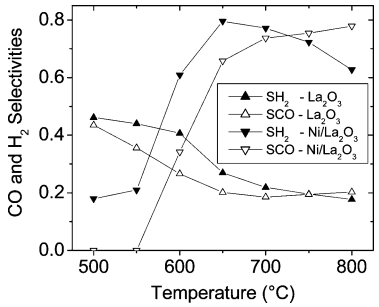

Figure 10. H_2 and CO selectivities versus temperature with four pellets of La_2O_3 and four pellets of $1.39Ni/La_2O_3$ at $\tau = 3$ s.

3.4. Mechanistic Considerations in a Perfectly Jet-Stirred reactor. *3.4.1. Catalyst Performances.* In this section, the experiments were conducted using four pellets of the $1.39Ni/La_2O_3$ catalyst at $\tau = 3$ s. Methane and oxygen conversions as a function of temperature are given in Figure 9. Conversions are very small in the absence of the catalyst, $X_{CH_4} = 3\%$ at 800 °C. It shows that the homogeneous POM reaction without the use of the catalyst would require high operating temperatures to get significant yields. Comparing conversions obtained with four La_2O_3 pellets and four Ni/La_2O_3 pellets shows the effect of nickel. At 700 °C, $X_{CH_4} = 11\%$ and $X_{O_2} = 25\%$ for La_2O_3, while it is 39% and 65%, respectively, with Ni/La_2O_3. It is also noteworthy that oxygen conversion keeps increasing regularly between 600 and 800 °C, while the methane conversion rate is lowered at higher temperatures. Interestingly, these trends are similar for both catalysts, that is, La_2O_3 and Ni/La_2O_3. The fact that $X_{O_2}/X_{CH_4} > 1$ clearly suggests that a total oxidation reaction occurs.

H_2 and CO selectivities are given in Figure 10 as a function of the temperature for La_2O_3 and $1.39Ni/La_2O_3$ catalysts. First, H_2 and CO selectivities show similar trends for a given catalyst. Both selectivities show a sharp increase between 550 and 650 °C when Ni/La_2O_3 is used, which is consistent with the fact that syngas production in the oxidative conversion of methane is thermodynamically favored at the higher temperatures. Moreover, the temperature range 550−650 °C corresponds to the reduction of NiO to Ni^0, the active site for the POM reaction. In contrast, both selectivities keep decreasing in this temperature range for the La_2O_3 catalyst. It was reported that La_2O_3 favors the total oxidation products, CO_2 and H_2O, to the detriment of the partial oxidation products, H_2 and CO, which would lead to a decrease of the syngas selectivity.[34] It is also interesting to note that, between 500 and 600 °C, selectivities are lower with Ni/La_2O_3 than with La_2O_3. This is due to the fact that in this temperature range only nickel oxide is present. And, it was effectively observed that in this temperature range CO_2 production is higher over Ni/La_2O_3 than over La_2O_3. Finally, it is noteworthy that, between 650 and 800 °C, H_2 selectivity decreases while CO selectivity increases.

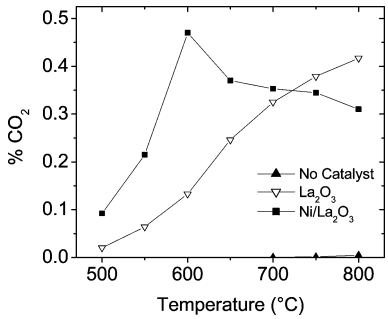

Figure 11. CO_2 production over La_2O_3 and $1.39Ni/La_2O_3$ as a function of temperature, at $\tau = 3$ s with four catalyst pellets.

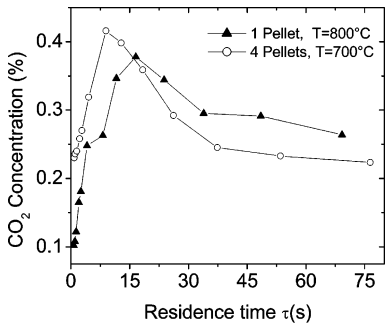

Figure 12. CO_2 production over $1.39Ni/La_2O_3$ as a function of residence time at two different conditions ($T = 800$ °C and one pellet and $T = 700$ °C and four pellets).

3.4.2. Side Products. Figure 11 reports CO_2 production over La_2O_3 and $1.39Ni/La_2O_3$ as a function of the temperature. CO_2 production is negligible in the absence of the catalyst. In the presence of the catalyst, the amount of CO_2 is on the same order of magnitude. But the main difference is that CO_2 production keeps increasing with the temperature over La_2O_3, while a maximum is observed at 600 °C over Ni/La_2O_3. Two main reasons can explain this behavior. First, as it was previously stated, the presence of NiO in the lower temperature range (500−600 °C) favors CO_2 production, whereas when NiO is reduced to Ni, CO is favored to the detriment to CO_2. Second, the dry reforming reaction $CH_4 + CO_2 \rightarrow 2CO + 2H_2$ and reverse water gas shift reaction $CO_2 + H_2 \rightarrow CO + H_2O$ may occur simultaneously with the partial oxidation of methane leading to CO_2 consumption.

Figure 12 shows CO_2 production over $1.39Ni/La_2O_3$ as a function of the residence time at two different conditions, $T =$ 800 °C with one pellet and $T = 700$ °C with four pellets. The main result is that a maximum is observed for both plots. When the residence time increases, the contact time increases proportionally. Furthermore, as the temperature is fixed, it is assumed that the nickel reduction degree is also constant for a given experiment. As a consequence, this result suggests that a sufficient contact time is required for the dry reforming reaction or the water gas shift reaction to occur significantly.

On the whole, C_2 production increases with the temperature over both La_2O_3 and Ni/La_2O_3 catalysts at a fixed residence

(32) Van Looij, F.; Geus, J. W. *J. Catal.* **1997**, *168*, 154−163.
(33) Campbell, R. A.; Szanyi, J.; Lenz, P.; Goodman, D. W. *Catal. Lett.* **1993**, *17*, 39−46.
(34) Hutchings, G. J.; Woodhouse, J. R.; Scurrell, M. S. *J. Chem. Soc., Faraday Trans.* **1989**, *85* (8), 2507−2523.

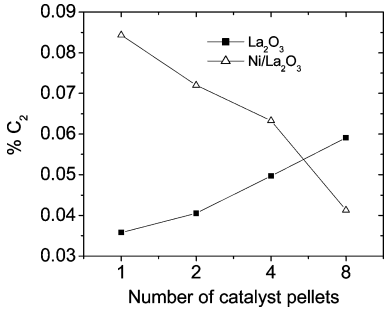

Figure 13. C_2 production versus the number of catalyst pellets at 800 °C and $\tau = 3$ s over La_2O_3 and 1.39Ni/La_2O_3.

time. C_2 production over La_2O_3 has been studied in our lab.[35] La_2O_3 was revealed to be an appropriate catalyst for the oxidative coupling reaction of methane, leading to the formation of C_2 compounds. It was shown on simulation and an experimental basis that C_2H_6 is first formed by recombination in the gas phase of $CH_3^\bullet$ radicals. Then, C_2H_6 may react with the surface to produce $C_2H_5^\bullet$ radicals. These radicals may be oxidized in the gas phase or may give C_2H_4. The following sequence can be written:

$$CH_4 \xrightarrow{surf} CH_3^\bullet \xrightarrow{+CH_3^\bullet} C_2H_6 \xrightarrow{surf} C_2H_5^\bullet \xrightarrow{gas} C_2H_4 \xrightarrow{surf} C_2H_3^\bullet \xrightarrow{gas} C_2H_2 \quad (9)$$

Figure 13 shows C_2 production at 800 °C and $\tau = 3$ s versus the number of La_2O_3 or Ni/La_2O_3 pellets. C_2 production increases with the number of La_2O_3 pellets, but it decreases with the number of Ni/La_2O_3 pellets. It suggests that nickel particles have a more disruptive effect on the chemical bonds C−H and C−C than the active sites of the La_2O_3 catalysts. Nickel has a beneficial effect for C_2 production at a low (catalyst surface/gas-phase volume) ratio but a detrimental effect at a higher ratio.

It is speculated that the adsorption of methane, ethane, and ethylene on nickel lead to the formation of surface carbon and hydrogen atoms. It was established that the intermediate species in the catalytic POM reaction are the $CH_{x,s}$ surface species.[11,16] It is therefore possible that surface coupling reactions occur:

$$CH_{x,s} + CH_{x,s} \rightarrow C_2H_{2x,g} \qquad (x = 3, 2, 1) \qquad (10)$$

Using the semiempirical bond-order conservation Morse potential approach, Au et al.[36] showed that this formation route of C_2 is possible but not significant over metallic nickel sites. Hu and Ruckenstein[11] suggested that CH_x oxidation is a faster pathway than its coupling.

Typically, La_2O_3 favors methyl radical production, leading to a higher production of C_2, while Ni/La_2O_3 favors methyl adsorption and its surface decomposition and surface oxidation, leading to a decrease of C_2 production with catalyst loading. Moreover, it is not excluded that C_2 compounds may adsorb and decompose into carbonated and hydrogenated compounds on nickel particles.

3.4.3. Experiments at Constant Contact Time but Variable Residence Times. In these experiments, when the catalyst amount was doubled, the flow rate was also doubled so that the contact time was unchanged while the residence time was divided by 2. The aim of this experiment is to check the relative importance of the surface reactions with respect to the gas-phase reactions.

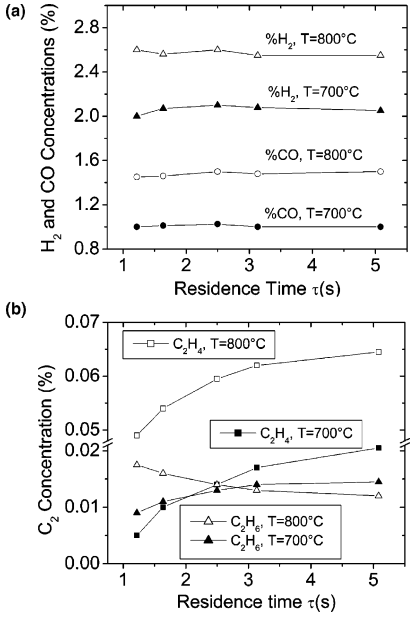

Figure 14. Outlet composition versus residence time at 700 and 800 °C ($t_c = 40$ mg s cm^{-3}). (a) H_2 and CO productions. (b) C_2H_6 and C_2H_4 productions.

Figure 14a shows H_2 and CO productions versus the residence time at 700 and 800 °C at $t_c = 0.04$ g s cm^{-3}. The outlet composition is constant despite the fact that the residence time is multiplied by 5. It means that the global reaction is driven by the heterogeneous reactions. Indeed, changing the residence time comes to changing the gas-phase volume of the reactor. As the results do not depend on the residence time, it means that the influence of the gas-phase reactions are small compared to the heterogeneous ones. Moreover, extrapolation of the corresponding curves when τ tends to 0 strongly suggests that H_2 and CO are primary products.

Figure 14b shows C_2H_4 and C_2H_6 productions at the same conditions. In this case, increasing the residence time favors the C_2 production. Homogeneous reactions have an influence on the C_2 production, and both heterogeneous and homogeneous reactions should be considered. As the aim of this work does not consist of producing C_2 compounds, it is recommended to minimize the gas-phase volume. In this way, the fixed-bed reactor is an appropriate reactor (section 3.5). Finally, it is noteworthy that, at 800 °C, the C_2H_6 concentration decreases with the residence time. This is due to its chemical decomposition into adsorbed species, oxygenated compounds, or C_2H_4.

3.5. Additional Catalytic Tests in a Fixed-Bed Reactor. The catalytic performances were tested in a fixed-bed reactor using the same catalyst 1.39Ni/La_2O_3 at $T = 700$ °C. The aim was to study the influence of the reactor type on the catalyst activity. Figure 15 shows the catalyst performances as a function of the contact time expressed in grams (of catalyst)•seconds per centimeter^3. The contact time was calculated at the standard conditions, that is, 25 °C and 1 atm. In these experiments, different amounts of the catalyst were used, 100 mg, 200 mg, and 300 mg. In this reactor, the residence time is very small as the gas-phase volume can be considered to be negligible.

The results reported in Figure 15 do not depend on the catalyst amount. In another words, catalytic activity is constant at a constant contact time. It means that there are no external diffusion limitations.

(35) Simon, Y.; Baronnet, F.; Côme, G.-M.; Marquaire, P.-M. *Stud. Surf. Sci. Catal*. **2004**, *147*, 571−576.

(36) Au, C.-T.; Liao, M.-S.; Ng C.-F. A. *J. Phys. Chem. A* **1998**, *102*, 3959−3969.

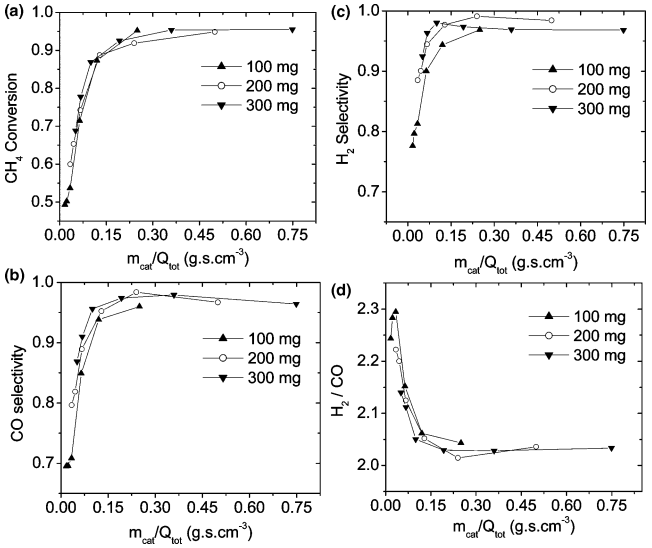

Figure 15. Catalytic performances of 1.39Ni/La_2O_3 in the FB using different amounts of the catalyst, 100 mg, 200 mg, and 300 mg, at 700 °C. (a) CH_4 conversion. (b) CO selectivity. (c) H_2 selectivity. (d) H_2/CO ratio.

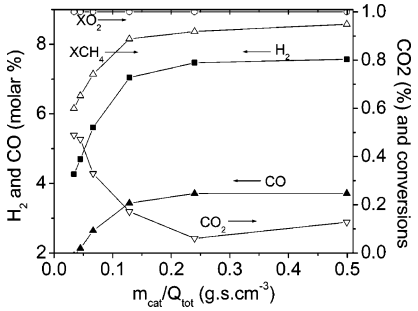

Figure 16. Products distribution versus contact time in the FB using 200 mg of 1.39Ni/La_2O_3 catalyst, at $T = 700$ °C.

Methane conversion and selectivities increase sharply between $t_c = 0$ and 0.15 g s cm^{-3}, while the H_2/CO ratio decreases. Oxygen conversion is equal to 100% over the whole range of contact time. At $t_c = 0.15$ g s cm^{-3}, methane conversion equals 90%, $S_{H_2} = 0.95$, $S_{CO} = 0.95$, and $H_2/CO = 2.04$. These results show that the Ni/La_2O_3 catalyst gives promising results for converting methane into syngas at the desired ratio for low-temperature Fischer−Tropsch synthesis. It shows also that high selectivities and yields can be attained even with low contents of Ni, as previously reported.[30,37] Moreover, most of the reported works related to catalytic tests with a nickel-based catalyst were carried out in a FB. Our results show that when a smaller amount of the catalyst but higher contact times are used, the FB is better than the PSR for catalytic performances.

Product distribution is given in Figure 16 when 200 mg of the catalyst is used. No C_2 compounds were detected. It is in agreement with what was previously stated in section 3.4.2: C_2 formation is favored by gas-phase reactions and low contact times. Moreover, as it was previously noticed in Figure 15a, methane conversion keeps increasing while oxygen conversion is total over the whole contact time range. It is usually expected that, when one of the reactants is totally consumed, the conversion of the other reactant is limited and cannot increase further. Figure 16 shows that syngas production increases with the contact time while CO_2 production decreases. Consequently,

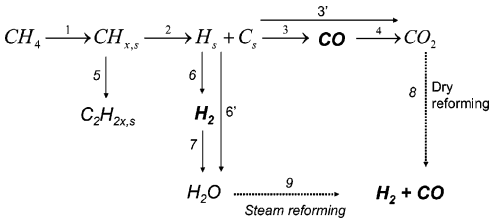

Figure 17. Simplified mechanism scheme of the main heterogeneous steps for the POM reaction.

it is believed that methane conversion increases thanks to the CO_2 reforming reaction, which becomes a reactant at higher contact times, in agreement with Swaan et al.[38] Hence, during the catalytic POM reaction, there is a direct syngas production, and as the extent of the reaction becomes more important, there is also an indirect syngas production via reforming reactions. In the direct mechanism, it is believed that CO is formed by an interaction with deposited carbon and $La_2O_2CO_3$ dispersed on the surface of Ni crystallites.[7,26,39] The production of CO is followed by the liberation of Ni sites for methane cracking, leading to a stable and good activity.[40] In fact, our results clearly suggest that short contact times give rise to the direct catalytic conversion of methane to syngas via the pyrolysis mechanism, while larger contact times give rise to the indirect mechanism. The influence of the contact time on the reaction scheme was shown by Bharadwaj and Schmidt.[41] It is believed that both direct and indirect mechanisms occur simultaneously during the POM reaction, in agreement with the work reported by Ruckenstein and Hu.[13]

A summary of the heterogeneous reaction mechanism, derived from the results obtained for the two reactor types, is given in Figure 17. The dashed arrows refer to the reforming reactions (steps 8 and 9), which mainly occur at higher contact times. Radical recombination and decomposition leading to C_2 formation are not represented. Methane dissociation occurs at the catalyst surface, and this dissociation may be helped by the existence of oxygen species.[42] From our results, we could not state whether the CO_2 was mainly formed by CO oxidation (steps 3 and 4) or directly as a primary product (step 3′). The same comment can be made for H_2O (see steps 6, 7, and 6′). The debate is still lively; the primary formation of CO_2 and H_2O is advocated by Basini et al.,[43] Chu et al.,[15] Lapszewicz and Jiang,[44] and Shen et al.,[45] while the formation of CO_2 via CO oxidation is advocated by Hu and Ruckenstein.[11,12] On the basis of the surface structure and the amount of available active oxygen species, both routes should be considered. Indeed, the direct formation of CO_2 as a primary product and the CO oxidation into CO_2 can occur contemporaneously, and it is difficult to differentiate both routes using common experimental techniques, such as the ones used in our work.

4. Conclusion

The partial oxidation of methane was investigated over Ni/La_2O_3 at a low nickel content ($x = 1.39$ wt %) using two

(37) Olsbye, U.; Tangstad, E.; Dahl, I. M. *Stud. Surf. Sci. Catal.* **1994**, *81*, 303−308.
(38) Swaan, H. M.; Rouanet, R.; Widyananda, P.; Mirodatos, C. *Stud. Surf. Sci. Catal.* **1997**, *107*, 447−453.
(39) Tsipouriari, V. A.; Verykios, X. E. *Catal. Today* **2001**, *64*, 83−90.
(40) Tsipouriari, V. A.; Verykios, X. E. *J. Catal.* **1998**, *179*, 292−299.
(41) Bharadwaj, S. S.; Schmidt, L. D. *J. Catal.* **1994**, *146* (1), 11−21.
(42) Luo, J. Z.; Yu, Z. L.; Ng, C. F.; Au, C. T. *J. Catal.* **2000**, *194*, 198−210.
(43) Basini, L.; D'Amore, M.; Fornasari, G.; Matteuzzi, D.; Sanfilippo, D.; Trifirò, F.; Vaccari, A. *Stud. Surf. Sci. Catal.* **1997**, *107*, 429−434.
(44) Lapszewicz, J. A.; Jiang, X.-Z. *Symp. Nat. Gas Upgrade II* **1992**, 252−260.
(45) Shen, S.; Li, C.; Yu, C. *Stud. Surf. Sci. Catal.* **1998**, *119*, 765−770.

different reactors, a perfectly jet-stirred reactor and a fixed-bed reactor. The catalyst exhibits good activity and excellent stability at temperatures ranging from 650 to 800 °C. At 700 °C, the H_2/CO ratio is 2, which is a desirable ratio for the low-temperature Fischer−Tropsch synthesis. The main conclusions are the following: (1) Selectivities and conversions depend highly on the reduction degree of nickel. It was shown that metallic nickel is active for syngas production, while nickel oxide favors the total oxidation products. (2) C_2 production is favored by gas-phase reactions where radical coupling and radical decomposition occur. (3) At low contact times, low temperatures, and low conversions, the reaction proceeds mainly via the direct mechanism. At higher contact times, it is believed that both the direct mechanism and the indirect mechanism, involving reforming reactions, occur at the same time.

Acknowledgment. The authors gratefully acknowledge the Région Lorraine and the Centre National pour la Recherche Scientifique for financial support. They also thank Maryse Bacri, Suzanne Libs, and Yvan Zimmermann for their help and assistance in the characterization studies.

EF0602729